Polymer Journal (2017) 49, 831–837

www.nature.com/pj

ORIGINAL ARTICLE

Role of molecular weight in shish-kebab formation during drawing by small-angle neutron and X-ray scattering

Toshiji Kanaya[1,2], Momoko Murakami[1], Tadahiko Maede[1], Hiroki Ogawa[1,3], Rintaro Inoue[1,4], Koji Nishida[1], Go Matsuba[5], Noboru Ohta[3], Shin-ichi Takata[6], Taiki Tominaga[7], Jun-ichi Suzuki[7], Young-Soo Han[8] and Tae-Hwan Kim[8]

The role of molecular weight during shish-kebab formation is an important issue in flow-induced polymer crystallization. In our previous study on the shish-kebab formation of polyethylene [*Macromolecules* 40, 3650–3654 (2007)], we have shown that ultrahigh molecular weight components are dominantly included in the shish. In contrast, in the same month (May 2007), a completely opposite experimental result was published for isotactic polypropylene [*Science* 316, 1014–1017 (2007)], wherein more low molecular weight components were found to be included in the shish than high molecular weight components. To understand this contradiction, we conducted small-angle neutron and X-ray-scattering experiments using blends of deuterated polyethylene and hydrogenated polyethylene with various molecular weights drawn just below the melting temperature at three drawing rates. We found that more low molecular weight components than high molecular weight components were included in the shish, even in polyethylene under such experimental conditions, and this tendency was enhanced as the drawing rate decreased. The results suggested that there are various mechanisms for shish-kebab formation that depend on the factors such as the type of flow fields, flow rate, type of polymer, temperature, molecular weight and molecular weight distribution.
Polymer Journal (2017) **49,** 831–837; doi:10.1038/pj.2017.65; published online 11 October 2017

INTRODUCTION

Polymer materials are crystallized under various kinds of flow during processing, such as fiber spinning, injection molding and extrusion. These flows affect the crystallization kinetics and the final morphology, thus determining the macroscopic properties of the material. In flow-induced crystallization processes, so-called shish-kebab structures are often observed, which consist of a long central core (shish: extended chain crystal) surrounded by lamellar crystals (kebabs). This structure was first observed by Mitsuhashi[1] and Pennings[2] in a polyethylene solution and was later observed in bulk polyethylene by Keller and coworkers[3] during development of ultrahigh modulus and ultrahigh strength fibers. The modulus and strength become higher as the number of shish-kebab structures increases.[4] Therefore, it is believed that shish-kebab structures are the structural origin of ultrahigh strength and modulus of fibers. Specifically, the oriented extended chain crystals (shish) must be the origin. Since then, extensive studies have been conducted to elucidate the shish-kebab morphology and mechanism of formation. The modulus and strength become higher when ultrahigh molecular weight components are added to the fibers,[5] thus indicating that the ultrahigh molecular weight components enhance the formation of the shish-kebab structures. These pioneering works were conducted more than 30 years ago, and at that time, it was hard to confirm the detailed shish-kebab structures at the molecular level.

As a consequence of recent developments in characterization techniques, extensive studies have been conducted on shish-kebabs by using rheo-small-angle and wide-angle X-ray scattering (SAXS and WAXS),[6–16] rheo-small-angle light scattering,[17,18] depolarized light scattering,[19,20] rheo-optical measurements[21–23] and small-angle neutron scattering (SANS).[24–26] Those studies have provided detailed information on the structure and formation mechanism of shish-kebabs.

In our previous paper,[20] we have examined the effects of high molecular weight components on shish-kebab formation. We applied a pulse shear flow to molten polyethylene and observed the subsequent crystallization process by using depolarized light scattering. When the PE sample included 3% of the ultrahigh molecular weight component, sharp streak-like scattering appeared normal to the flow

[1]Institute for Chemical Research, Kyoto University, Kyoto-fu, Japan; [2]Material and Life Science Division, J-PARC, Institute of Material Structure Science, High Energy Accelerator Research Organization (KEK), Ibaraki-ken, Japan; [3]Japan Synchrotron Radiation Research Institute, Hyogo-ken, Japan; [4]Research Reactor Institute, Kyoto University, Osaka-fu, Japan; [5]Department of Polymer Science and Engineering, Faculty of Engineering, Yamagata University, Yamagata-ken, Japan; [6]Neutron Science Section, Material and Life Science Division, J-PARC Center, JAEA, Ibaraki-ken, Japan; [7]Research Center for Neutron Science and Technology, Comprehensive Research Organization for Science and Society (CROSS), Ibaraki-ken, Japan and [8]Korea Atomic Energy Research Institute, Daejon, South Korea
Correspondence: Professor T Kanaya, Institute for Chemical Research, Kyoto University, Gokashi, Uji, Kyoto-fu 61-0011, Japan.
E-mail: kanaya@scl.kyoto-u.ac.jp
Received 24 July 2017; revised 26 August 2017; accepted 28 August 2017; published online 11 October 2017

direction just after application of the pulse shear flow, thus suggesting the formation of bundles of shish structures or precursors of shish structures. However, the PE sample without ultrahigh molecular weight components did not show any streak-like scattering under the same flow and temperature conditions. The results strongly suggest that the shish formation was enhanced by the addition of the ultrahigh molecular weight component. We have also investigated the role of ultrahigh molecular weight components on shish-kebab formation in drawn PE[24] by using a PE blend of 97.2 wt% deuterated PE (d-PE) and 2.8 wt% hydrogenated PE (h-PE) with an ultrahigh molecular weight. The blend film was drawn just above the melting temperature, and SAXS and SANS measurements were carried out after drawing process. The idea of the experiment was as follows. SAXS contrast originates from differences in the electron density; thus, h-PE and d-PE could not be distinguished. In contrast, SANS contrast originates from differences in the scattering length density; therefore, h-PE and d-PE could be distinguished. If the ultrahigh molecular weight component (h-PE) were distributed homogeneously in the sample with the shish-kebab structure, the SAXS and SANS patterns would be nearly identical. However, if the ultrahigh molecular component (h-PE) formed a shish, the SANS contrast would be considerably enhanced. Streak-like scattering normal to the drawing direction was observed only in the SANS pattern but not in the SAXS pattern.[24] We concluded that the ultrahigh molecular weight component (h-PE) was mainly included in the shish.

However, in the same month (May 2007), a completely opposite experimental result was published with blends of deuterated and hydrogenated isotactic polypropylene and by Sumitomo Chem. Co. group.[25] Their findings indicated that more of the low molecular weight component was included in the shish than the high molecular weight component. The results from both of the studies were reliable, thus suggesting that there are other unknown mechanisms for shish-kebab formation that depend on the crystallization conditions, such as the crystallization temperature and nature of the flow. In the present work, we propose a possible scenario for shish-kebab formation within PE in which the low molecular weight component, rather than the high molecular weight component, is the major constituent of the shish, to confirm that there is another shish-kebab formation mechanism for PE. To confirm the scenario, SANS and SAXS experiments on drawn PE blends of d-PE and h-PE with various molecular weights were conducted. Notably, we herein define the shish-kebab structure, consisting of extended chain crystals (shish) surrounded by lamellar crystals (kebabs), at the nanometer scale morphologically, irrespective of the formation mechanism.

EXPERIMENTAL PROCEDURES

Samples

d-PE with a weight average molecular weight of $M_w = 600\,000$ and molecular weight distribution of $M_w/M_n = 2$ and h-PE with various molecular weights of $M_w = 58\,000$, $300\,000$ and $2\,000\,000$ and $M_w/M_n = 8 \sim 12$ were used in this experiment. The blends of d-PE and h-PE were prepared as follows: the two types of PE were dissolved in hot *o*-dichlorobenzene with an antioxidant reagent (2,6-*t*-butyl-*p*-cresole) to form a homogeneous solution at 170 °C. After the solution was heated at 170 °C for 3 h, it was poured into ethanol to precipitate the blend. Then, the blend sample was filtered through *o*-dichlorobenzene and rinsed with ethanol. The precipitate was vacuum-dried at 40 °C for 12 h. The dried samples were hot-pressed at 180 °C for 10 min and quenched rapidly in a mixture of ice and water. Films with a thickness of ~0.5 mm were obtained, and dumbbell-shaped specimens were cut out. The concentration of h-PE in the blend was 3 wt%. The nominal melting temperature of the films determined by DSC measurements was 132 °C for all blends. The heating rate for the DSC measurements was 5 °C min^{-1}. The blend films were drawn at three drawing rates of 6 μm s^{-1}, 400 μm s^{-1} and 2.4 cm s^{-1} at 125 °C with a drawing machine made in the laboratory.

Measurements

SANS measurements were carried out using two machines. The first machine used was the TAIKAN[27] installed at the spallation neutron source in the Material and Life Science Experimental Facility at J-PARC in Tokai, Japan. Using TAIKAN, we conducted two dimensional measurements in a low Q ($=4\pi\sin\theta/\lambda$; 2θ being scattering angle) range from 1×10^{-2} to 3 $Å^{-1}$. The other SANS instrument used was a 40 m SANS machine [28] at the HANARO reactor in Daejeon, Korea. In the 40 m SANS measurements, the scattering vector Q ranged from 2×10^{-3} to 1×10^{-1} $Å^{-1}$. Combining the data from the two instruments, Q ranged from 2×10^{-3} to 3 $Å^{-1}$ in this study. This wide Q range is a distinct feature of this experiment. The scattering data obtained in each instrument were corrected according to the standard procedure in the corresponding facility but not converted to the absolute intensity.

SAXS and WAXS measurements were conducted using BL40B2 installed at SPring-8, Nishiharima, Japan. For the SAXS measurements, a CCD camera (C4880: Hamamatsu Photonics K.K., Hamamatsu, Japan) with an image intensifier was used as the detector system. The Q ranges in the SAXS and WAXS measurements were 7×10^{-3} to 1×10^{-1} $Å^{-1}$ and 6×10^{-1} to 3 $Å^{-1}$, respectively.

The scattering measurements were conducted at room temperature with the drawn PE blend samples. The draw ratio λ, which is defined as l/l_0 (l_0 and l being the initial and final lengths, respectively), was 7.0 at the beam position for all samples.

RESULTS AND DISCUSSION

On the basis of our previous experimental results,[26] we considered a possible scenario for shish-kebab formation in which the low molecular weight component, rather than the high molecular weight component, was the major constituent of the shish. *In situ* SANS and SAXS measurements were conducted for a blend of d-PE ($M_w = 600\,000$; 97 wt%) and h-PE ($M_w = 2\,000\,000$; 3 wt%) during a drawing process with a drawing rate of 6 μm s^{-1} at 125 °C, which is just below the melting temperature ($=132$ °C).[26] Among the many aspects of shish-kebab formation during the drawing process discussed previously,[26] the key finding was as follows: At the beginning of the drawing process (at a draw ratio of 2.4, as shown in Figure 1 ((a)1 and (a)3), we observed streak-like scattering normal to the drawing direction only in the SANS pattern, thus suggesting that the high molecular weight components formed the shish.

These results probably occurred because the high molecular weight component was easily stretched, owing to the entangled network. During the drawing process, the two-spot (oblate) pattern observed along the meridian direction due to the presence of kebabs (stacked lamellar crystals) gradually decreased and finally disappeared near a drawing ratio of 5. At the drawing ratio of 8.0, no kebab scattering was observed. The decrease in the scattering intensity of the kebab is shown in Figure 1(b). These results suggested that the polymer chains included in the kebab (lamellar crystals) were merged into a shish, and the kebab disappeared. The same disappearance phenomenon has also been previously observed in transmission electron microscopy experiments.[29] We suspect that the merging process of polymer chains into a shish from a kebab may be more difficult for higher molecular weight components than for lower molecular weight components because the higher molecular weight chains are entangled with other chains and go through several lamellar crystals, as shown in the cartoon in Figure 2. In the scenario, the kebab is formed not from the precursor amorphous components but from precursor lamellar crystals in the original film. Nevertheless, we use the term 'kebab' to describe the 'oriented lamellae' because shish-kebab is defined morphologically in the paper.

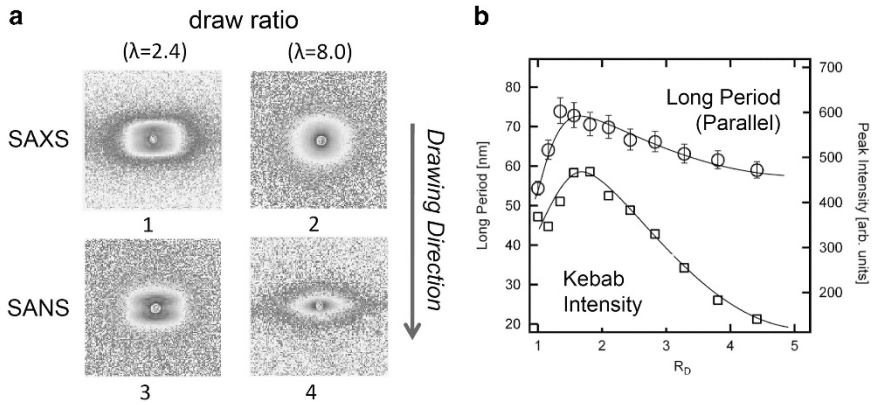

Figure 1 (**a**)1–4: 2D SANS [(**a**)1 and (**a**)2] and SAXS [(**a**)3 and (**a**)4] patterns of a blend of d-PE with $M_w = 600\,000$ (97 wt%) and h-PE with $M_w = 2\,000\,000$ (3 wt%) during drawing at 125 °C. The draw ratios are 2.4 for (**a**)1 and (**a**)3 and 8.0 for (**a**)2 and (**a**)4. (**b**) time evolution of the long period and peak intensity (or kebab intensity) during the drawing process. Reproduced from ref. 26. A full color version of this figure is available at *Polymer Journal* online.

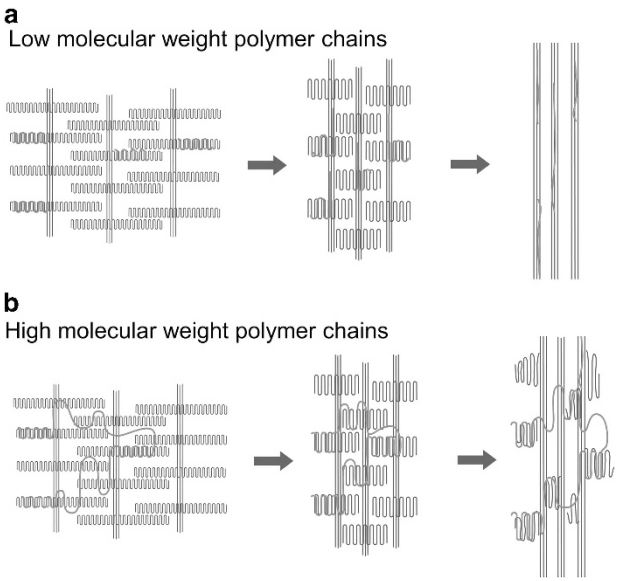

Figure 2 An illustration of the expected structural development during drawing. (**a**) and (**b**) show the merging processes into a shish from a kebab for low and high molecular weight chains, respectively. The red curves show labeled polymer chains. A full color version of this figure is available at *Polymer Journal* online.

In this proposed mechanism, polymer chains must slide along the chain axis in the kebab (lamellar crystals). Such a sliding motion of the PE chains occurs only during the rotor phase (so-called α_c relaxation).[30] In addition, in this mechanism, the relaxation rate of the sliding motion of the polymer chains must be faster than the drawing rate. Otherwise, the polymer chains cannot escape from the lamellar crystals to merge into the shish. It is difficult to measure the relaxation rates quantitatively, which depend on the lamellar size as well as the reentry mechanism of the polymer chains into the lamellae. In any case, we expect that the slower the drawing rate, the more the polymer chains are included in the shish. On the basis of the above considerations, we sought to confirm the scenario by using SANS and SAXS measurements on drawn films of d-PE and h-PE with various molecular weights. From the experimental results, we had to distinguish between the two types of PE at the nanometer scale. Therefore, we used SANS and SAXS measurements for this experiment.

Figure 3 shows the 2D SAXS and SANS patterns for the drawn PE blend films. The 2D SAXS patterns showed weak two-spot patterns along the drawing direction corresponding to the distance between the kebabs (or lamellar crystals). The 2D SAXS patterns were very similar, thus suggesting that the small amount of added h-PE (3 wt%) did not affect the whole structure of the PE blends and functioned as a tracer. In contrast, in the 2D SANS patterns, streak-like scattering was observed normal to the drawing direction. Streak-like scattering corresponding to scattering from the h-PE was observed in addition to the two-spot pattern, thus suggesting that the shish mainly consisted of h-PE. Notably, the two spots in the 2D SANS pattern are not very clear, owing to the larger Q scale compared with that of the 2D SAXS patterns, but they can be clearly seen in the 1D profiles in Figure 4. At the same drawing rate, the streak-like scattering was enhanced as the molecular weight of the h-PE decreased. These results suggested that the low molecular weight component was more easily merged into the shish than the high molecular weight component. The merger between the polymer chains to form a shish should have been hindered by the high molecular weight component, because the high molecular weight chains were more entangled and went through a larger number of lamellar crystals than the low molecular weight chains. Furthermore, for the same molecular weight of h-PE (for example, $M_w = 58\,000$), the streak-like scattering was enhanced as the drawing rate decreased. As the drawing rate decreased, the polymer chains may have had sufficient time to slide out of the lamellar crystals. Therefore, the low drawing rate enhanced the merging of the polymer chains into a shish. The observed results qualitatively supported the picture predicted in the scenario.

To carry out a quantitative analysis, we evaluated the 1D SAXS and SANS intensities in the directions normal and parallel to the drawing direction. The intensities in the azimuthal angle ranging from −7.5 to 7.5° (normal) and from 82.5 to 97.5 ° (parallel) were integrated for each 2D SAXS and SANS pattern. In Figure 4, the normal and parallel intensities are plotted. The SAXS and SANS intensities were adjusted so that both of the X-ray and neutron Bragg peak intensities and the intensities at $Q = 0.4$–$0.6\ \text{Å}^{-1}$ were the same because the structure fluctuations were very small near $Q = 0.4$–$0.6\ \text{Å}^{-1}$.[31]

In the 1D SAXS and SANS profiles, strong Bragg peaks from the (110) and (200) planes were observed at 1.5 and 1.6 Å^{-1}, respectively,

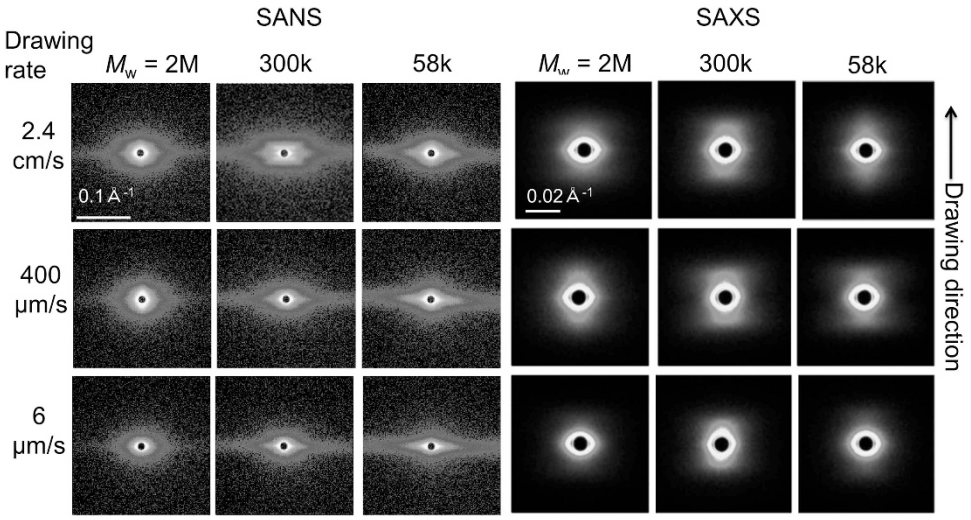

Figure 3 2D SAXS and SANS patterns for the drawn PE blends containing 3 wt% h-PE with different molecular weights. The draw ratio is 7.0 for all samples. A full color version of this figure is available at *Polymer Journal* online.

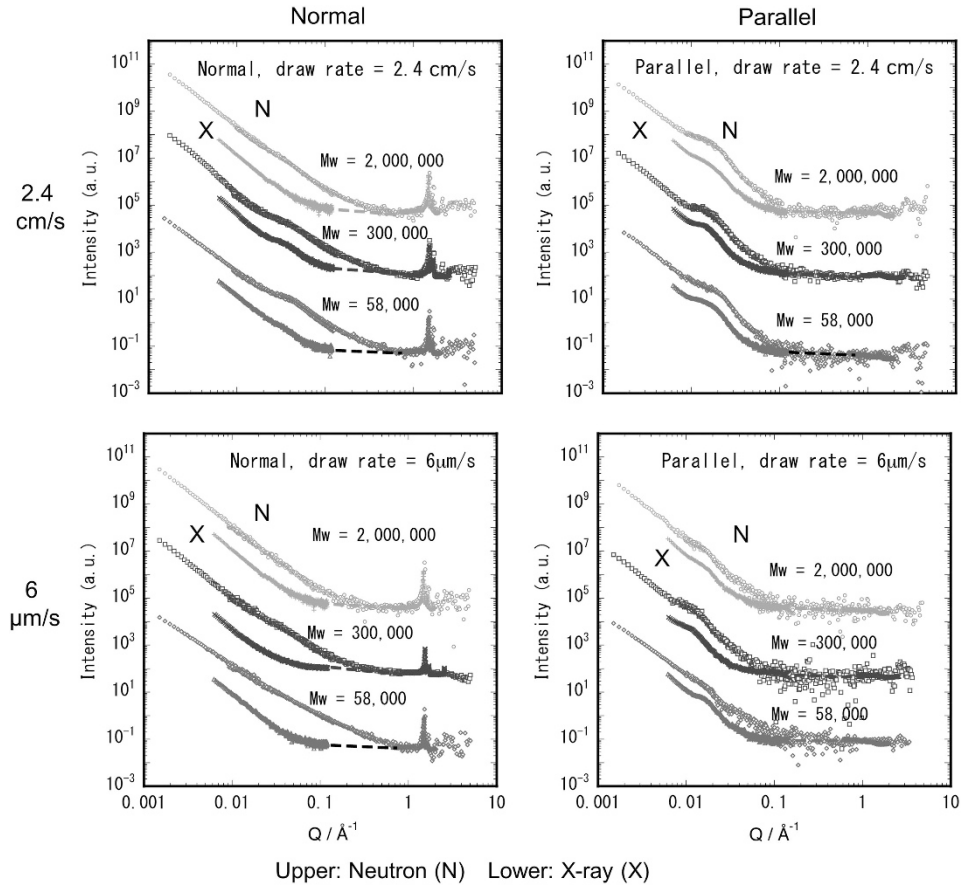

Figure 4 SAXS and SANS intensities in the directions normal and parallel to the drawing direction for the PE blends containing 3 wt% h-PE with different molecular weights. In the figures, the upper curves are the SANS intensities, and the lower curves are the SAXS intensities. A full color version of this figure is available at *Polymer Journal* online.

in the normal direction but not in the parallel direction, thus showing that the crystals (mainly kebabs) were highly oriented. In the parallel direction, broad peaks corresponding to the distance between the kebabs were observed near $Q = 0.015$ Å^{-1} in both the SAXS and SANS, thus indicating that the kebabs mainly consisted of d-PE. Comparison of the intensities in the normal direction between the drawing rates of 2.4 cm s^{-1} and 6 μm s^{-1} indicated broad peaks owing to the kebabs for 6 μm s^{-1} but very weak shoulders for 2.4 cm s^{-1}. This difference indicated that the merging of the polymer chains into the shish was more pronounced in the slower drawing rate,

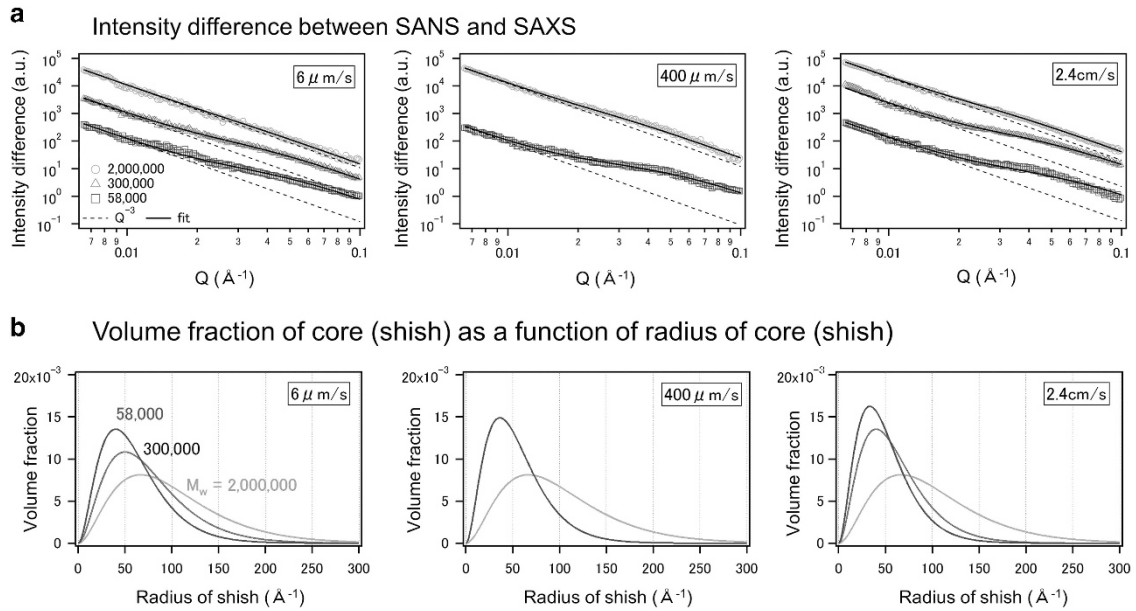

Figure 5 (**a**) Intensity differences between the SANS and SAXS results in the normal direction for the PE blends containing h-PE with different molecular weights. The solid curves are the results of the fits using the multicore-shell cylinder model. The dashed lines show the contributions of the large shell. (**b**) Volume fraction of the core (shish) as a function of the radius of the core (shish). A full color version of this figure is available at *Polymer Journal* online.

as predicted by the scenario. The differences in the intensities between the SAXS and SANS increased with decreasing molecular weight. This result also supported the prediction that the low molecular weight components would more easily merge into the shish than the high molecular weight components.

As mentioned in our previous paper,[24] the SANS contrast in the present samples arises from the scattering length density difference due to the mass density difference and the scattering length density difference between the hydrogen (H) and deuterium (D). It was assumed that the correlation function of the mass density and the correlation function of the H/D density could be decoupled because the fraction of h-PE was very small (3 wt%). Furthermore, it was assumed that the streak-like scattering normal to the drawing direction mainly originated from the h-PE, and the other scattering included only d-PE, because the scattering contrast of the streak-like scattering in the SANS was very strong compared with the contrast in the SAXS in the low Q range below $\sim 0.1\,\text{Å}^{-1}$ (see Figure 4). Under these assumptions, the form factor for the streak-like scattering normal to the drawing direction was obtained as the difference between the SANS and SAXS intensities. The intensity differences are shown in Figure 5 for the PE blends containing h-PE with different molecular weights and drawing rates. During the subtraction process, we ignored the incoherent scattering contribution from the hydrogen atoms in the h-PE because it was very small in the measurement results.

According to our previous paper,[24] the intensity difference in the small-angle region below $\sim 0.1\,\text{Å}^{-1}$ can be considered to be a form factor of row structures at the microscale including shish structures at the nanoscale, especially in the normal direction. In principle, the intensity difference in the parallel direction could also be considered a form factor. However, the subtraction of the SAXS intensity from the SANS intensity did not work well because of the strong scattering due to the kebab correlation. Therefore, the data in the parallel direction were not used for further analyses to evaluate the form factors of the row structures and/or the shish structures.

The same multicore-shell cylinder model used in the previous report[24] was applied to analyze the intensity differences in the normal direction. In this model, several extended chain crystal cores (shish structures) are included in a large shell cylinder (row structure). The illustration of the model can be found in Figure 5 in reference 24. In the model, the cross term between the cores and the shell is negligible because of the small amount of h-PE. Ignoring the cross term between two cores and the cross term between the core and the shell, the scattering intensity can be approximated by

$$I(\boldsymbol{Q}) = [V_{shell}(\rho_{shell} - \rho_0)A_{shell}(\boldsymbol{Q}, R_{shell}, H)]^2 + [nV_{core}(\rho_{core} - \rho_{shell})A_{core}(\boldsymbol{Q}, R_{core}, H)]^2 \quad (1)$$

where n is number of the core cylinders in a shell cylinder; $A(\boldsymbol{Q}, R, H)$ is the scattering amplitude of a cylinder with a length of $2H$ and a radius of R;[32] V_{shell}, V_{core}, R_{shell} and R_{core} are the shell and core volumes and the shell and core radii, respectively; and ρ_{shell}, ρ_{core} and ρ_0 are the scattering length densities of the shell, core and d-PE matrix, respectively. In this calculation, we calculated $\rho_{core} = \rho_{CH}\rho_{shell}$, assuming that the shells were homogeneously distributed in the system with a degree of crystallinity of 0.6. During the fitting, the distribution of the core (shish) radii was taken into account. The results of the fitting are shown as black solid lines in Figure 5, in which the shell contributions are also indicated by dashed lines. The fitting results show that the multicore-shell cylinder model is appropriate for describing the row structure and shish structure. In all of these fittings, the contribution from the shish (core) in the Q range above $\sim 0.01\,\text{Å}^{-1}$ was necessary as well as the shell (shown as dashed lines in Figure 5) to fit the experimental curve. In addition, the contribution from the shish to the intensity difference increased with decreasing molecular weight of the h-PE. These results suggested that the row structure includes the shish, and the content of the low molecular weight component is higher than that of the high molecular weight component within the shish.

The volume fraction of the shish (Figure 5(b)) showed the broad distribution of shish radii. As the molecular weight of the h-PE increased, the radius of the shish increased. For example, at the drawing rate of 6 μm/s, the average values of the shish radii were 1.3, 2.7 and 2.7 nm for $M_w = 58\,000$, 300 000 and 2 000 000, respectively.

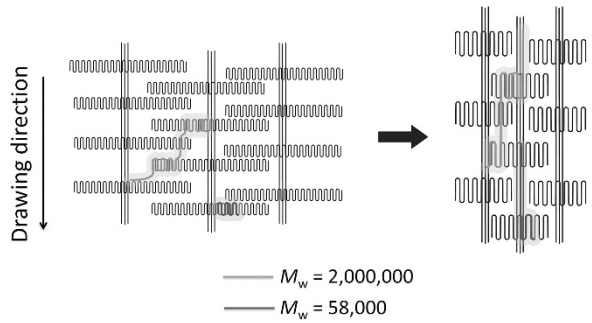

Figure 6 Illustration explaining why the core (shish) radius is larger for the high molecular weight h-PE ($M_w = 2\,000\,000$) than for the low molecular weight h-PE ($M_w = 58\,000$). The red and blue lines represent h-PE with $M_w = 2\,000\,000$ and $M_w = 58\,000$, respectively. A full color version of this figure is available at *Polymer Journal* online.

We wondered whether this result might be explained within our scenario proposed in Section 2. When high molecular weight polymer chains merge into the shish, some parts of the polymer chains may remain outside the shish because they are entangled with other chains and enter through several lamellar crystals. The remaining part of the high molecular weight chains outside the shish would exhibit a large apparent shish radius. In contrast, in the case of the low molecular weight polymer chains, the chains are more likely to be completely merged into the shish and exhibit relatively smaller shish radii than the high molecular weight components. The apparent shish radii for the high and low molecular weight chains are illustrated in Figure 6. Thus, the observed results can be qualitatively explained with the scenario.

In the present experimental work, it was found that the content of the low molecular weight PE component was higher than that of the high molecular weight component in the shish in the case of slow drawing at a temperature below the melting temperature. We consider that this result may have been due to α_c relaxation.[30] As mentioned in the introduction, this work was motivated by two contrary experimental results on the flow-induced crystallization of PE and iPP. One study[24] has indicated that the high molecular weight component is the major component of the shish in PE crystallized during drawing just above the melting temperature, whereas the other[25] study has indicated that the low molecular weight components are the major component in the shish for iPP processed with an extruder. Though we have not studied iPP or other flow conditions, it is clear that there are various mechanisms for shish-kebab formation that depend on factors such as the type of flow field, flow rate, type of polymer, temperature, molecular weight and molecular weight distribution. In some cases, high molecular weight components would form the shish, but in other cases, low molecular weight components would form the shish.

SUMMARY

In this study, we conducted *ex situ* SANS and SAXS measurements by using blends of d-PE with $M_w = 600\,000$ and h-PE with $M_w = 58\,000$, 300 000 and 2 000 000 (3 wt%). The PE films were drawn below the melting temperature at three drawing rates to determine the effects of the molecular weights on the shish-kebab formation. This study was motivated by two contradicting experimental results regarding shish-kebab formation in PE and iPP, although experimental conditions such as the flow type and temperature were different. One study[24] has found that the high molecular weight component is mainly included in the shish. In contrast, the other study[25] has found that the low molecular weight component rather than the high molecular weight component is included more in the shish. The experimental present results were qualitatively consistent with a scenario in which the low molecular weight components were included more in the shish than the high molecular weight components, and as the drawing rate decreased, the low molecular weight components were dominantly included in the shish. We cannot discuss the results in terms of iPP or other flow conditions because we did not carry out such experiments. However, the present experimental results suggest that there are various shish-kebab formation mechanisms that depend on various factors, such as the type of flow field, flow rate, type of polymer, temperature, molecular weight and molecular weight distribution. In some cases, the high molecular weight components would form the shish, but in other cases, the low molecular weight components would form the shish.

CONFLICT OF INTEREST

The authors declare no conflict of interest.

ACKNOWLEDGEMENTS

This research was financially supported by a Grant-in-Aid for Scientific Research (A) (No. 24245045) from the Japan Society for the Promotion of Science (JSPS) and Photon and Quantum Basic Research Coordinated Development Program from the Ministry of Education, Culture, Sports, Science and Technology, Japan. The neutron experiment at the Materials and Life Science Experimental Facility of the J-PARC was performed with a user program (Proposal No. 2013A0056, 2013B0011 and 2014B0048). The synchrotron radiation experiments were performed at the BL40B2 of SPring-8 with the approval of the Japan Synchrotron Radiation Research Institute (JASRI) (Proposal No. 2013A1408, 2013B1345 and 2014B1256).

1 Mitsuhashi, S. On the crystalline textures of polyethylene grown under rotational flow in xylene solution. *Bull. Text. Res. Inst.* **66**, 1–9 (1963).
2 Pennings, A. J. & Kiel, A. M. Fractionation of polymers by crystallization from solution, III. On the morphology of fibrillar polyethylene crystals grown in solution. *Colloid Polym. Sci.* **205**, 160–162 (1965).
3 Odell, J. A., Grubb, D. T. & Keller, A. A new route to high modulus polyethylene by lamellar structures nucleated onto fibrous substrates with general implications for crystallization behavior. *Polymer* **19**, 617–626 (1978).
4 Keller, A., Kolnaar, H. W. H. Flow-induced orientation and structure formation. In *Processing of Polymers*. Vol. 18 (eds Meijer H. E. H.) 189–268 (Wiley-VCH, New York, NY, USA (1997).
5 Bashir, Z., Odell, J. & Keller, A. High modulus filaments of polyethylene with lamellar structure by melt processing; The role of the high molecular weight component. *J. Mater. Sci.* **19**, 3713–3725 (1984).
6 Samon, J. M., Schultz, J. M., Hsiao, B. S., Seifert, S., Stribeck, N., Gurke, I., Collins, G. & Saw, C. Structure development during the melt spinning of polyethylene and poly (vinylidene fluoride) fibers by in situ synchrotron small- and wide-angle X-ray scattering techniques. *Macromolecules* **32**, 8121–8132 (1999).
7 Samon, J. M., Schultz, J. M., Wu, J., Hsiao, B. S., Yeh, F. & Kolb, R. Study of the structure development during the melt spinning of nylon 6 fiber by on-line wide-angle synchrotron X-ray scattering techniques. *J. Polym. Sci.: Part B: Polym. Phys.* **37**, 1277–1287 (1999).
8 Somani, R. H., Hsiao, B. S., Nogales, A., Srinivas, S., Tsuo, A. H., Sics, I., Balta-Calleja, J. & Ezquerra, T. A. Structure development during shear flow-induced crystallization of i-PP: In-situ small-angle X-ray scattering study. *Macromolecules* **33**, 9385–9394 (2000).
9 Schultz, J. M., Hsiao, B. S. & Samon, J. M. Structural development during the early stages of polymer melt spinning by in-situ synchrotron X-ray techniques. *Polymer* **41**, 8887–8895 (2000).
10 Samon, J. M., Schultz, J. M., Hsiao, B. S., Wu, J. & Khot, S. Structure development during melt spinning and subsequent annealing of polybutene-1 fibers. *J. Polym. Sci.: Part B: Polym. Phys.* **38**, 1872–1882 (2000).
11 Samon, J. M., Schultz, J. M., Hsiao, B. S., Khot, S. & Johnson, H. R. Structure development during the melt spinning of poly(oxymethylene) fiber. *Polymer* **42**, 1547–1559 (2001).
12 Nogales, A., Somani, R. H., Hsiao, B. S., Srinivas, S., Tsuo, A. H., Balta-Calleja, J. & Ezquerra, T. A. Shear-induced crystallization of isotactic polypropylene with different molecular weight distributions: in situ small- and wide-angle X-ray scattering studies. *Polymer* **42**, 5247–5256 (2001).

13 Somani, R. H., Hsiao, B. S., Nogales, A., Fruitwala, H., Srinivas, S. & Tsuo, A. H. Structure development during shear flow induced crystallization of i-PP: In situ wide-angle X-ray diffraction study. *Macromolecules* **34**, 5902–5909 (2001).
14 Somani, R. H., Young, L., Hsiao, B. H., Agarwal, P. K., Fruitwala, H. A. & Tsuo, A. H. Shear-induced precursor structures in isotactic polypropylene melt by in-situ rheo-SAXS and rheo-WAXD studies. *Macromolecules* **35**, 9096–9104 (2002).
15 Somani, R. H., Yang, L. & Hsiao, B. S. Precursors of primary nucleation induced by flow in isotactic polypropylene. *Physica A* **304**, 145–157 (2002).
16 Yang, L., Somani, R. H., Sics, I., Hsiao, B. H., Kolb, R., Fruitwala, H. & Ong, C. Shear-induced crystallization precursor studies in model polyethylene blends by in-situ rheo-SAXS and rheo-WAXD. *Macromolecules* **37**, 4845–4859 (2004).
17 Pogodina, N. V., Lavrenko, V. P., Srinivas, S. & Winter, H. H. Rheology and structure of isotactic polypropylene near the gel point: Quiescent and shear-induced crystallization. *Polymer* **42**, 9031–9043 (2001).
18 Elmoumni, A., Winter, H. H., Waddon, A. J. & Fruitwala, H. Correlation of material and processing time scales with structure development in isotactic polypropylene crystallization. *Macromolecules* **36**, 6453–6461 (2003).
19 Fukushima, H., Ogino, Y., Matsuba, G., Nishida, K. & Kanaya, T. Crystallization of polyethylene under shear flow as studied by time resolved depolarized light scattering. Effects of shear rate and shear strain. *Polymer* **46**, 1878–1885 (2005).
20 Ogino, Y., Fukushima, H., Matsuba, G., Takahashi, N., Nishida, K. & Kanaya, T. Effects of high molecular weight component on crystallization of polyethylene under shear flow. *Polymer* **47**, 5669–5677 (2006).
21 Kumaraswamy, G., Issaian, A. M. & Kornfield, J. A. Shear-enhanced crystallization in isotactic polypropylene. 1. Correspondence between in situ rheo-optics and ex situ structure determination. *Macromolecules* **32**, 7537–7547 (1999).
22 Kumaraswamy, G., Verma, R. K., Issaian, A. M., Wang, P., Kornfield, J. A., Yeh, F., Hsiao, B. & Olley, R. H. Shear-enhanced crystallization in isotactic polypropylene Part 2. Analysis of the formation of the oriented 'skin.'. *Polymer* **41**, 8934–8940 (2000).
23 Kumaraswamy, G., Kornfield, J. A., Yeh, F. & Hsiao, B. Shear-enhanced crystallization in isotactic polypropylene. 3. Evidence for a kinetic pathway to nucleation. *Macromolecules* **35**, 1762–1769 (2002).
24 Kanaya, T., Matsuba, G., Ogino, Y., Nishida, K., Shimizu, H. M., Shinohara, T., Oku, T., Suzuki, J. & Otomo, T. Hierarchic structure of shish-kebab by neutron scattering in a wide Q range. *Macromolecules* **40**, 3650–3654 (2007).
25 Kimata, S., Sakurai, T., Nozue, Y., Kasahara, T., Yamaguchi, N., Karino, T., Shibayama, M. & Kornfield, J. A. Molecular basis of the shish-kebab morphology in polymer crystallization. *Science* **316**, 1014–1017 (2007).
26 Matsuba, G., Ito, C., Zhao, Y., Inoue, R., Nishida, K. & Kanaya, T. In situ small-angle X-ray and neutron scattering measurements on a blend of deuterated and hydrogenated polyethylenes during uniaxial drawing. *Polym. J.* **45**, 293–299 (2013).
27 Shinohara, T., Takata, S. I., Suzuki, J. I., Oku, T., Suzuya, K., Aizawa, K., Arai, M., Otomo, T. & Sugiyama, M. Design and performance analyses of the new time-of-flight smaller-angle neutron scattering instrument at J-PARC. *Nucl. Instr. Meth. Phys. Res. A* **600**, 111–113 (2009).
28 Han, Y., Choi, S., Kim, T., Lee, C. & Kim, H. Design of 40M SANS instrument at HANARO, Korea. *Physica B* **386**, 1177–1179 (2006).
29 Ohta, Y., Murase, H. & Hashimoto, T. Structural development of ultra-high strength polyethylene fibers: Transformation from kebabs to shishs through hot-drawing process of gel-spun fibers. *J. Polym. Sci. B Polym. Phys.* **48**, 1861–1872 (2010).
30 Hu, W. G., Boeffel, C. & Schmidt-Rohr, K. Chain flips in polyethylene crystallites and fibers characterized by dipolar 13C NMR. *Macromolecules* **32**, 1611–1619 (1999).
31 Wiegand, W. & Ruland, W. Density fluctuations and the state of order of amorphous polymers. *Prog. Colloid Polymer Sci.* **66**, 355–366 (1979).
32 Shibayama, M., Nomura, S., Hashimoto, T. & Thomas, E. L Asymptotic behavior and Lorentz factor for small-angle elastic scattering profiles from preferentially oriented asymmetric bodies. *J. Appl. Phys.* **66**, 4188–4197 (1989).